

Variable-Speed Wind Turbine Coupled Three-Phase Self-Excited Induction Generator Voltage Regulation Scheme with Static VAR Compensator Controlled by PI Controller

Tarek Ahmed, Katsumi Nishida, Shinji Sato, Shinichro Nagai, Eiji Hiraki and Mutsuo Nakaoka
The Graduate School of Science and Engineering, Yamaguchi University
Yamaguchi, Japan

Abstract-In this paper, a PI controlled feedback closed-loop voltage regulation scheme of the three-phase squirrel cage rotor self-excited induction generator (SEIG) driven by a variable-speed prime mover (VSPM) such as a wind turbine is designed on the basis of the static VAR compensator (SVC) and discussed in experiment for the promising stand-alone power independent conditioner. The simulation and experimental results of the three-phase SEIG with the simple SVC controller for its stabilized voltage regulation prove the practical effectiveness of the additional SVC control loop scheme including the PI controller with fast response characteristics and steady-state performance improvements.

Keywords: Three-Phase Self-Excited Induction Generator, Variable-Speed Wind Turbine, Static VAR Compensator

1. Introduction

From an earth environment point of view, solar photovoltaic and wind turbine power generation systems have attracted special interests for renewable and sustainable energy in the rural region. Of these, the AC generators driven by the wind turbine are typically divided into two; synchronous generator and induction generator, which has widely used for the utility AC power interactive and stand-alone power systems. The three-phase induction machine with squirrel cage rotor or wound rotor could work as a three-phase induction generator either it is connected to a utility AC power distribution line supply or operate in the self-excitation mode with the terminal excitation capacitor bank[1-5]. This paper presents the performance evaluations together with the experimental results of the closed loop PI controller based voltage regulation of the three-phase self-excited induction generator (SEIG) driven directly by a variable-speed prime mover (VSPM) using the static VAR compensator; SVC.

2. Voltage Regulation Implementation

The schematic power conditioning system diagram of the three-phase SEIG voltage regulation scheme used the SVC controlled by a PI compensator in the feedback

control loop scheme is illustrated in Fig.1. The 4 poles, 220V, 2kW, star connected stator winding, three-phase squirrel cage rotor SEIG is designed for supplying, either a resistive load or an inductive load. The three-phase induction generator excited by the SVC composed of the fixed excitation capacitor bank FC in parallel with the thyristor switched capacitor TSC and the thyristor controlled reactor TCR.

3. Static VAR Controller For SEIG Voltage Regulation

The fundamental component of the inductive current through the TCR is defined as[1],

$$I_{TRCI} = B_{TCR}(\sigma)V_t \quad (1)$$

where B_{TCR} is the equivalent inductive susceptance of TCR and is defined as a function of the conduction angle σ as,

$$B_{TCR}(\sigma) = \frac{\sigma - \sin \sigma}{\pi X_{TCR}} \quad (2)$$

$$\text{where } \alpha + \frac{\sigma}{2} = \pi \quad (3)$$

The control variable of the thyristor triggering delay angle α is between $\pi/2$ and π . Observing eqn.(3), the control range of the conduction angle σ corresponding to the control variable of α will be between π and zero. The Laplace transformation of the output signal $E_c(s)$ of the PI controller is indicated by,

$$E_c(s) = \left(K_p + \frac{K_i}{s} \right) (V_{ref}(s) - V_{tr}(s)) \quad (4)$$

where $V_{ref}(s)$, $V_{tr}(s)$ are the Laplace transformation of the reference voltage and rectified voltage proportional to the terminal voltage of the three-phase SEIG, respectively, K_p and K_i are the Proportional gain and Integral gain of the PI controller, respectively. The above equation can be expressed in the discrete form as follow,

$$E_c(k) = E_c(k-1) + (K_p + T_s K_i) [V_{ref}(k) - V_{tr}(k)] - K_p [V_{ref}(k-1) - V_{tr}(k-1)] \quad (5)$$

where $[V_{ref}(k) - V_{tr}(k)]$ is the terminal voltage error at the sampling time k , $[V_{ref}(k-1) - V_{tr}(k-1)]$ is the error signal at the sampling time $(k-1)$, T_s is the sampling period(sec).

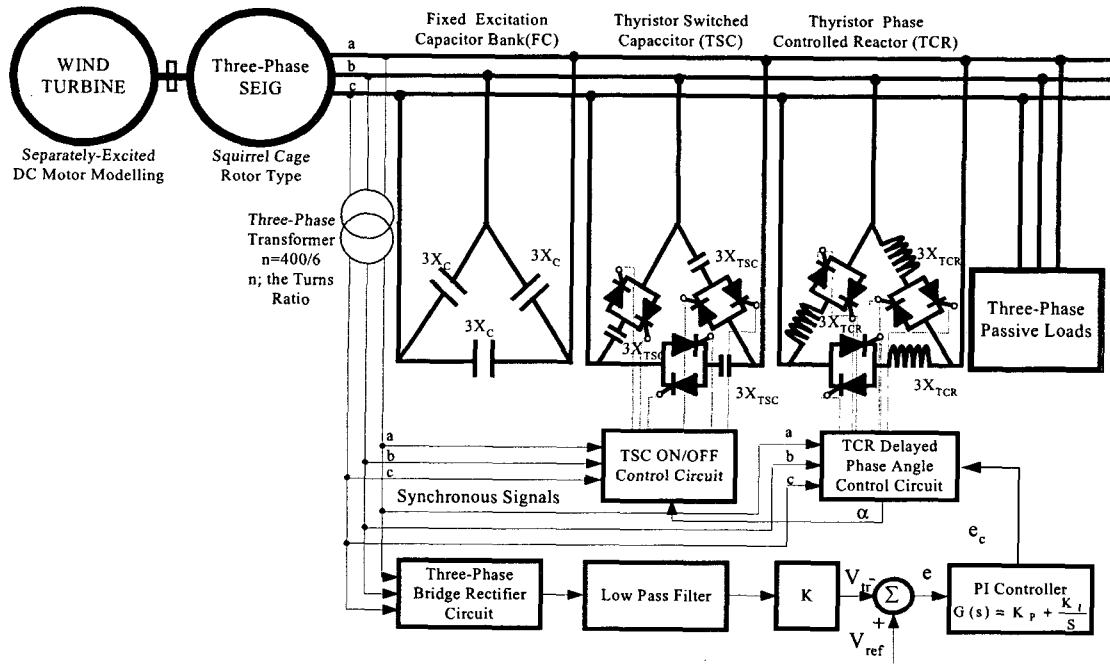


Fig.1 Schematic system configuration of SEIG driven by VSPM with SVC controlled by FI controller

4. Torque-Speed Characteristics of VSPM

The mechanical output power P_m of the VSPM; a separately-excited dc motor used in experiment is defined as,

$$P_m = (\tau_o - v_o v) \omega_s v \quad (6)$$

where v is the per unit speed ($v=N/N_s$), N and N_s are the rotor speed and the synchronous speed in (rpm), respectively. τ_o , v_o and ω_s respectively are the torque coefficient, speed coefficient and the synchronous angular speed and defined as[1]

$$\tau_o = \frac{K_t \phi_m V_a}{R_a}, \quad v_o = \frac{2\pi K_t^2 \phi_m^2}{60 R_a} N_s \quad \text{and} \quad \omega_s = \frac{2\pi N_s}{60}$$

where K_t is the torque constant, ϕ_m is the field flux per pole of the dc motor in wb, V_a is the armature voltage in volt and R_a is the armature resistance in ohm.

5. Voltage Regulation Analysis of SEIG with SVC

The per-phase approximate electro-mechanical equivalent circuit in the frequency domain of the three-phase SEIG excited by the SVC is depicted in Fig.2. The equivalent susceptance $B_{TCR}(\sigma)$ of the TCR as a function of its conduction angle σ and the capacitive reactance X_{TSC} of the TSC which is switched on under the conditions of the terminal voltage of the three-phase SEIG is less than the reference voltage; 220 and the conduction angle $\sigma=0$ of the TCR or the triggering delayed angle $\alpha=\pi$ are connected in parallel with the fixed excitation reactance X_C .

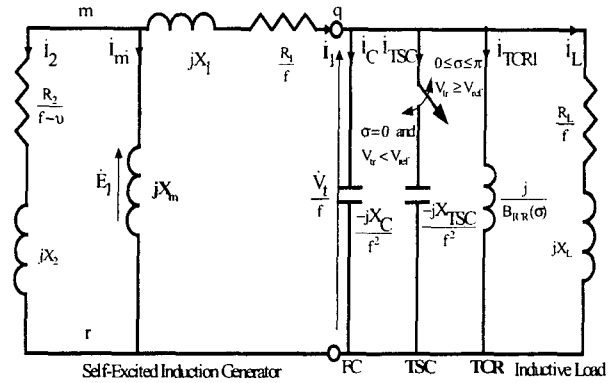


Fig.2 Per-phase approximate electro-mechanical equivalent circuit of the three-phase SEIG with SVC

The rotor current I_2 referred to the stator side of the three-phase SEIG can be expressed as,

$$I_2 = \frac{(f - v)E_1}{\sqrt{R_2^2 + (f - v)^2 X_2^2}} \quad (7)$$

where E_1 is the air gap voltage per phase, R_2 and X_2 are the resistance and the leakage reactance of the rotor winding referred to the stator winding side in ohm, respectively. The per unit frequency $f=F/50.0$ where F is the output frequency of the three-phase SEIG. The term $(f-v)$ is usually very small. Therefore, the term $(f-v)^2 X_2^2$ can be

neglected with respect to R_2^2 . Thus, the above equation of the rotor current is reduced to the following equation,

$$I_2 = \frac{(f - v)E_1}{R_2} \quad (8)$$

The three-phase induction machine mechanical input power P_i can be written as[2],

$$P_i = -3I_2^2 \frac{R_2}{(f - v)} \left(\frac{v}{f}\right) \quad (9)$$

By substituting I_2 in eqn.(8) into eqn.(9) and making a mechanical power balance from an energy conversion principle through equating the eqn.(9) to eqn.(6). The per unit speed v can be obtained as follows:

$$v = \frac{(\tau_0 + \frac{3E_1^2}{R_2\omega_s})f}{v_0f + \frac{3E_1^2}{R_2\omega_s}} \quad (10)$$

By applying the nodal admittance approach on the per-phase approximate equivalent circuit of the three-phase SEIG with SVC depicted in Fig.2, the following equation can be written as follows,

$$(\dot{Y}_{mr} + \dot{Y}_m + \dot{Y}_r)E_1 = 0 \quad (11)$$

But E_1 does not equal to zero for the generated terminal voltage, the following nodal admittance relationship yields,

$$(\dot{Y}_{mr} + \dot{Y}_m + \dot{Y}_r) = 0 \quad (12)$$

\dot{Y}_{mr} , \dot{Y}_m and \dot{Y}_r can be represented as,

$$\dot{Y}_{mr} = \frac{1}{\left(\frac{R_L}{f} + jX_L\right)(-jX_{SVC}) + \frac{R_1}{f} + jX_1} \quad (13)$$

where $X_{SVC} = \frac{X_C + X_{TSC}}{f^2 - (X_C + X_{TSC})B_{TCR}(\sigma)}$

$$\dot{Y}_m = -\frac{j}{X_m} \quad (14)$$

and $\dot{Y}_r = \frac{1}{\left[\frac{R_2}{f - v} + jX_2\right]} \quad (15)$

where R_1 and X_1 are the resistance and the leakage reactance of the stator winding in ohm, respectively, R_L and X_L are the load resistance and reactance in ohm, respectively and $X_C = (1/100\pi C; 50\text{Hz})$. Where C is the terminal excitation capacitance in farad and v is defined by eqn.(10). Equating the sum of the imaginary terms in eqn.(12) to zero, the magnetizing reactance X_m can be obtained by,

$$X_m = \frac{1}{B_r + B_{mr}} \quad (16)$$

and then equating the sum of the real terms of eqn.(12) to zero, the 10th order polynomial function as a function in the per unit frequency f can be arranged as follow,

$$\begin{aligned} & Y_{10}f^{10} + Y_9f^9 + Y_8f^8 + Y_7f^7 \\ & + Y_6f^6 + Y_5f^5 + Y_4f^4 + Y_3f^3 \\ & + Y_2f^2 + Y_1f + Y_0 = 0 \end{aligned} \quad (17)$$

where B_r , B_{mr} and the eleven coefficients Y_0 to Y_{10} are derived and given in Appendix . From eqn.(17) the per-unit frequency f can be determined using Newton Raphson method and then substitute the per-unit frequency f into eqn.(16) to calculate the magnetizing reactance X_m . The air gap voltage E_1 is evaluated from the magnetization characteristic obtained experimentally from the no-load test of the three-phase induction machine and defined as the relationship between the air gap voltage E_1 and the magnetizing reactance X_m . The magnetizing characteristic is represented by the following equation.

$$E_1 = \begin{cases} 207.2 - 3.773 X_m & X_m \leq 24.2 \\ 541.7 - 17.79 X_m & 24.2 \leq X_m \leq 26.5 \\ 0 & X_m \geq 26.5 \end{cases} \quad (18)$$

Observing Fig.2, the terminal voltage per phase of the three-phase SEIG can be defined as,

$$V_t = fE_1 \frac{\left| \frac{1}{\dot{Y}_{mr}} - \left(\frac{R_1}{f} + jX_1\right) \right|}{\left| \frac{1}{\dot{Y}_{mr}} \right|} \quad (19)$$

6. Experimental Results and Discussions

Due to the wind turbine prime mover speed changing and load fluctuating, the terminal voltage of the three-phase SEIG is unregulated and changed. The SVC voltage regulation compensator connected at the three-phase SEIG terminals is used to regulate and stabilize its terminal voltage as suggested in Fig.1. The digital computer simulation results and the experimental results of the three-phase SEIG terminal voltage response and the TCR triggering delay angle response due to the inductive load variations are shown respectively, in Fig.3, Fig.4 with SVC composed of FC in parallel with TCR, and then in Fig.5, Fig.6 with SVC composed of FC in parallel with TCR and TSC. In experiment, the TSC is switched on manually by observing the terminal voltage response of the three-phase SEIG

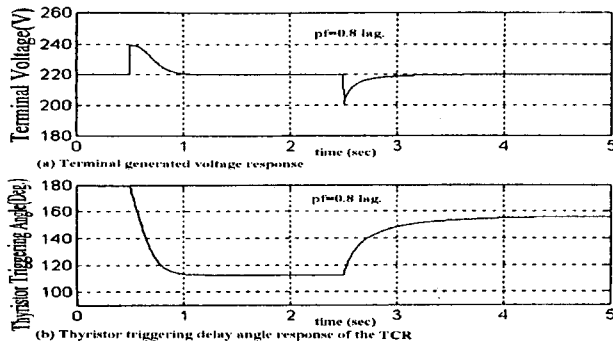


Fig.3 Digital terminal voltage and TCR triggering angle using FC and TCR

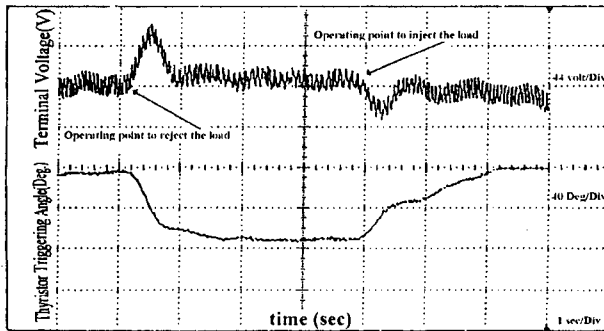


Fig.4 Experimental terminal voltage and TCR triggering angle responses using FC and TCR

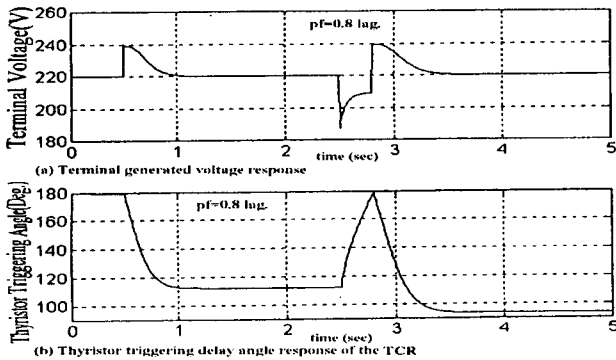


Fig.5 Digital terminal voltage and TCR triggering angle responses using FC, TSC and TCR

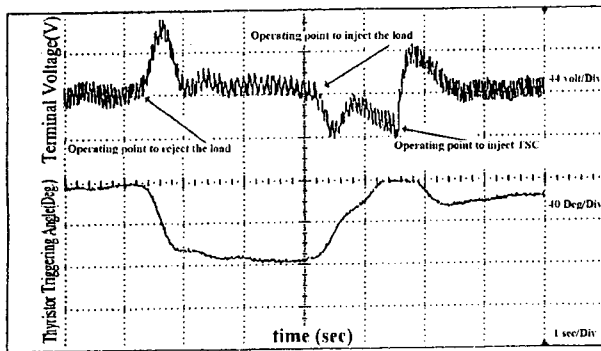


Fig.6 Experimental terminal voltage and TCR triggering angle responses using FC, TSC and TCR

7. Conclusions

The present paper has developed a SVC controlled system for the voltage regulation of the three-phase SEIG. The external disturbances as inductive load variations have been applied to build and test the proposed SVC controlled system. The responses of the three-phase SEIG have been determined in terms of its terminal voltage and the TCR triggering delay angle responses and validated the feasible effectiveness of the SVC controlled implementation. The measured responses of the operating performances of the three-phase SEIG could give good agreements with the simulation ones.

References

- [1] IEEE Special Stability Controls Working Group Report, "Static VAR Compensator Models for Power Flow and Dynamic Performance Simulation", IEEE Transactions on Power Systems, Vol.9, No.1 February, 1994.
- [2] S.Rajakarvna and R.Bonert, "A Technique for The Steady state Analysis of Self-Excited Induction Generator with Variable Speed", IEEE Trans. on Energy Conversion, Vol.8, No.4 pp.757-761, December, 1993.
- [3] Marcos S. Miranda, Renato O. C. Lyra and Selenio R. Silva, "An Alternative Isolated Wind Electric Pumping System Using Induction Machines", IEEE Trans. on Energy Conversion, Vol.14, No.4 pp.1611-1616, December, 1999.
- [4] E. Suarez and G. Bortolotto, "Voltage-Frequency Control of A Self-Excited Induction generator", IEEE Trans. on Energy Conversion, Vol.14, No.3 pp.394-401, September, 1999.
- [5] R. Leidhold, G. Garcia and M.I. Valla, "Induction generator Controller Based on the Instantaneous Reactive Power Theory", IEEE Trans. on Energy Conversion, Vol.17, No.3 pp.368-373, September, 2002.

Appendix

$$\dot{Y}_r = G_r + jB_r, \quad \dot{Y}_r = \frac{(A_0 + A_1f + A_2f^2)f + j(Q_0 + Q_1f + D_2f^2)f^2}{T_0 + T_1f + T_2f^2 + T_3f^3 + T_4f^4}$$

where $T_0=G_0^2$, $T_1=2G_0G_1$, $T_2=G_1^2+G_2^2X_2^2$, $T_3=2G_2G_3X_2^2$, $T_4=G_3^2X_2^2$, $A_0=G_0G_2$, $A_1=G_1G_2+G_0G_3$, $A_2=G_1G_3$, $Q_0=-G_2^2X_2$, $Q_1=-2G_2G_3X_2$, $Q_2=-G_3^2X_2$

where $G_0=3E_1^2/\omega_s$, $G_1=u_0R_2$, $G_2=-\tau_0$ and $G_3=u_0$, $R_1=0.52$ ohm, $X_1=1.01$ ohm, $R_2=0.52$ ohm, $X_2=1.01$ ohm, $\tau_0=120$, $u_0=133$, $N_s=1500$ rpm,

$$\dot{Y}_{mr} = G_{mr} + jB_{mr},$$

$$\dot{Y}_{mr} = \frac{(D_0 + D_2f^2 + D_4f^4 + D_6f^6)f + j(C_0 + C_2f^2 + C_4f^4 + C_6f^6)f^2}{P_0 + P_2f^2 + P_4f^4 + P_6f^6 + P_8f^8}$$

Where $F_0=-R_1X_cR_lB_{TCR}$, $F_2=X_cX_l+X_1X_c+R_lR_1+X_1X_cX_lB_{TCR}$, $F_4=-X_1X_l$,

$T_{01}=-R_1X_c-X_cR_l-R_1X_cX_lB_{TCR}-X_1X_cR_lB_{TCR}$, $T_{21}=R_1X_l+X_1R_l$,

$P_0=F_0^2$, $P_2=2F_0F_2+T_{01}^2$, $P_4=2F_0F_4+F_2^2+2T_{01}T_{21}$, $P_6=2F_2F_4+T_{21}^2$, $P_8=F_4^2$,

$D_0=B_{TCR}F_0$, $D_2=R_lF_0-B_{TCR}X_cR_lF_2-X_cT_{01}(X_lB_{TCR}+1)$,

$D_4=R_lF_2-B_{TCR}X_cR_lF_4-X_cT_{21}(X_lB_{TCR}+1)+X_lT_{01}$, $D_6=R_lF_4+X_lT_{21}$,

$C_0=T_{01}B_{TCR}X_cR_l-X_cF_0(X_lB_{TCR}+1)$,

$C_2=-R_lT_{01}+B_{TCR}X_cR_lT_{21}+X_lF_0-X_cF_2(X_lB_{TCR}+1)$,

$C_4=-T_{21}R_l+X_lF_2-X_cF_4(X_lB_{TCR}+1)$, $C_6=F_4X_l$,

$Y_0=T_0D_0+A_0P_0$, $Y_1=T_1D_0+A_1P_0$, $Y_2=T_0D_2+T_2D_0+A_0P_2+A_2P_0$,

$Y_3=T_1D_2+T_3D_0+A_1P_2$, $Y_4=T_0D_4+T_2D_2+T_4D_0+A_0P_4+A_2P_2$,

$Y_5=T_1D_4+T_3D_2+A_1P_4$, $Y_6=T_0D_6+T_2D_4+T_4D_2+A_0P_6+A_2P_4$,

$Y_7=T_1D_6+T_3D_4+A_1P_6$, $Y_8=T_2D_6+T_4D_4+A_0P_8+A_2P_6$,

$Y_9=T_3D_6+A_1P_8$, $Y_{10}=T_4D_6+A_2P_8$